Materials Letters 213 (2018) 303–305

Contents lists available at ScienceDirect

Materials Letters

journal homepage: www.elsevier.com/locate/mlblue

In-situ synchrotron X-ray radiography observation of primary Al_2Cu intermetallic growth on fragments of aluminium oxide film

Feng Wang [a,*], Dmitry Eskin [a], Thomas Connolley [b], Chuangnan Wang [c], Billy Koe [c], Andrew King [d], Christina Reinhard [b], Jiawei Mi [c]

[a] Brunel Centre for Advanced Solidification Technology (BCAST), Brunel University London, Uxbridge UB8 3PH, UK
[b] Diamond Light Source Ltd, Harwell Science & Innovation Campus, Didcot OX11 0DE, UK
[c] School of Engineering & Computer Science, University of Hull, Hull, East Yorkshire HU6 7RX, UK
[d] Synchrotron SOLEIL, L'Orme des Merisiers, Saint-Aubin, BP 48 91192, Gif-sur-Yvette Cedex, France

ARTICLE INFO

Article history:
Received 9 August 2017
Received in revised form 23 October 2017
Accepted 19 November 2017
Available online 21 November 2017

Keywords:
Solidification
Synchrotron X-ray radiography
Metals and alloys
Intermetallic phase
Structure refinement
Oxide film

ABSTRACT

While using synchrotron X-ray radiography for studying ultrasonic melt processing, the growth of the primary Al_2Cu intermetallic phase on fragments of aluminium oxide film during solidification of a hypereutectic Al-35% Cu alloy was observed in-situ and in real time with adequate spatial and temporal resolution. This provides the first direct evidence for the nucleation of a primary phase on oxide particles during solidification of real metallic alloys. Comparison of the primary Al_2Cu intermetallics grown in the melt with and without fragments of aluminium oxide film reveals considerable refinement, which demonstrates that the enhanced nucleation of a primary phase on oxide particles promotes structure refinement.

1. Introduction

Impurity particles, particularly oxide inclusions, existing in the melt of many metals and alloys, have long been considered as potential heterogeneous nucleation sites for the primary phases during solidification [1,2]. Furthermore, it has been suggested that enhancing the heterogeneous nucleation of primary phase on oxide particles by various means such as ultrasonic melt processing [3,4] and intensive melt shearing [5,6] during solidification can promote refinement of primary phase, leading to beneficial microstructure changes. Using dedicated solidification experiments, it has been demonstrated that aluminium and magnesium oxide particles are indeed potent heterogeneous nucleation substrates for Al and Mg grains, respectively [5–7]. In addition, aluminium oxide particles have been observed at or near the centre of primary Al_3Ti and Al_3Zr intermetallic particles in Al alloys [8–10]. Similarly, magnesium oxide particles have been observed at the centre of primary Al_8Mn_5 intermetallic particles in Mg alloys [8]. Although these results seem quite convincing, they were all obtained from microstructural analysis on samples after solidification and therefore represent indirect evidence. As a result, direct evidence to conclusively substantiate the nucleation of a primary phase on oxide particles during solidification has always been desirable, yet very challenging to obtain.

Using synchrotron X-ray radiography [11–16] during ultrasonic melt processing (USP) of Al alloys, we for the first time captured in situ and in real time the distinct primary Al_2Cu intermetallic growth on fragments of indigenous aluminium oxide film in a hypereutectic Al-35% Cu alloy with sufficient spatial and temporal resolution. The composition throughout the paper is in weight percentage unless otherwise stated.

2. Experimental setup and methods

The synchrotron experiments were carried out at the Pression Structure Imagerie par Contraste à Haute Énergie (PSICHÉ) beamline of Synchrotron SOLEIL, France [17]. A schematic of the experimental setup at the beamline is shown in Fig. 1. The hypereutectic Al-35% Cu alloy was first melted in a custom-made quartz crucible inside a two-zone furnace. The temperatures of top and bottom halves were set as 630 °C and 600 °C respectively. The temperature of 600 °C for the bottom half was chosen to ensure that the alloy

* Corresponding author.
E-mail address: feng.wang@brunel.ac.uk (F. Wang).

https://doi.org/10.1016/j.matlet.2017.11.090
0167-577X/

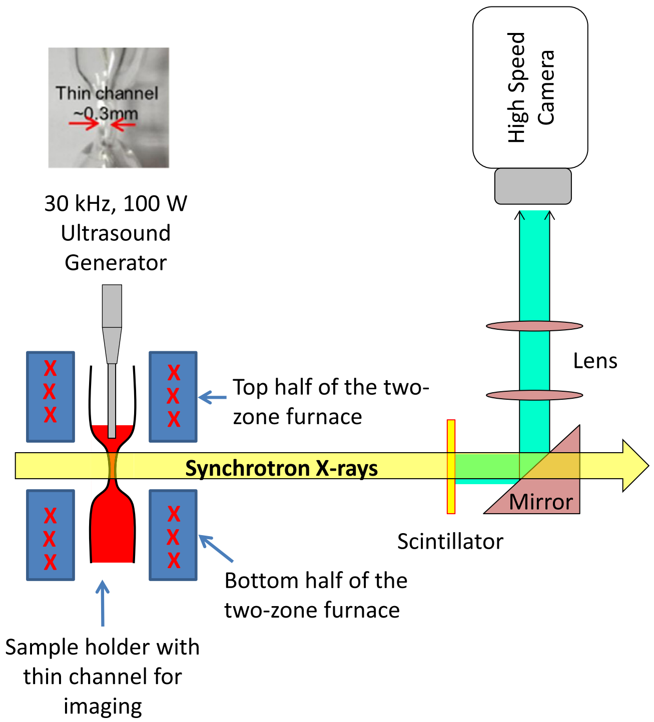

Fig. 1. A schematic of the experimental setup at the PSICHÉ beamline of SOLEIL.

was fully molten because the liquidus temperature of Al-35% Cu alloy is 554 °C. Furthermore, the temperature of 630 °C for the top half was chosen to establish a positive thermal gradient (~1 K/mm) in the melt. This positive thermal gradient was needed to force the primary Al_2Cu intermetallic to grow from bottom to top in order to facilitate the insertion of the sonotrode. The custom-made quartz crucible was a 10 mm inner diameter tube, flattened in the middle to a ~300 µm thickness as shown in the inset of Fig. 1. After both halves of the furnace reached their target temperatures, they were held at these temperatures for ~5 min to ensure the alloy was fully molten and also to allow sufficient aluminium oxide film growth on the melt surface. Following that, the solidification process was started by setting both the top and bottom furnace halves to a cooling rate of ~2 K/min. The growth of primary Al_2Cu intermetallic was recorded using a Vision Research Miro 310 M high speed camera attached to the X-ray imaging optics (5× magnification) at the beamline. The size of the field of view was 5120 × 2624 µm^2 and the nominal pixel resolution was 4 µm/pixel. When the primary Al_2Cu intermetallic growth front appeared at the bottom of the imaging field of view, a niobium sonotrode (1 mm in diameter) driven by a Hielscher UP100H ultrasonic transducer was inserted into the melt from the top to apply USP, and hence to introduce oxide particles from the surface oxide film. The ultrasonic transducer power was 100 W with a frequency of 30 kHz and the USP duration was around 5 s. After the ultrasonic transducer was switched off and the sonotrode was lifted out of the melt, the subsequent solidification of primary Al_2Cu intermetallic was recorded at 1 frame per second (fps). A detailed experimental procedure can be found elsewhere [13,18].

3. Results and discussion

An image sequence extracted from a radiography video recording the typical primary Al_2Cu intermetallic growth on the fragments of oxide film is shown in Fig. 2. The corresponding video is supplied in the online version of this publication. We recommend viewing the video because the moving images clearly show the details described in the text. Radiography recording was started at the moment when the sonotrode was lifted out of the melt so that no forced convection is present. The first frame of the recording is defined as time $t = 0$ s. As shown in Fig. 2(a), the dark phase is the primary Al_2Cu intermetallic and the grey matrix is the alloy melt. The light grey particles marked by numbers are fragments of aluminium oxide film. In total, **10** fragments of aluminium oxide film were successfully introduced to the melt by USP in this experiment and they remained rather stationary in the field of view which facilitated observation of their effect on intermetallic growth. The identification of those fragments as aluminium oxide film was based on their X-ray attenuation compared to that of the melt and the analysis is detailed in the Supplementary Appendix due to the page limit.

As solidification proceeded, slight growth of the primary Al_2Cu intermetallic was noticed on the *No. 1* and *No. 2* fragments of oxide film at the bottom left corner in Fig. 2(b). Following that, distinct growth of the primary Al_2Cu intermetallic on the fragments of oxide film (*No. 1, 2, 4, 5, 6, 7, 8, 9* and *10*) was manifested in Fig. 2(c) and (d). An enlarged image of the intermetallic growth on the fragments of oxide film *No. 5* and *No. 6* is shown in Fig. 2(f) for better clarity. As the growth on these fragments of oxide film continued, the primary Al_2Cu intermetallic particles finally impinged on each other as shown in Fig. 2(e), leaving no space for further growth. The average intermetallic length is measured

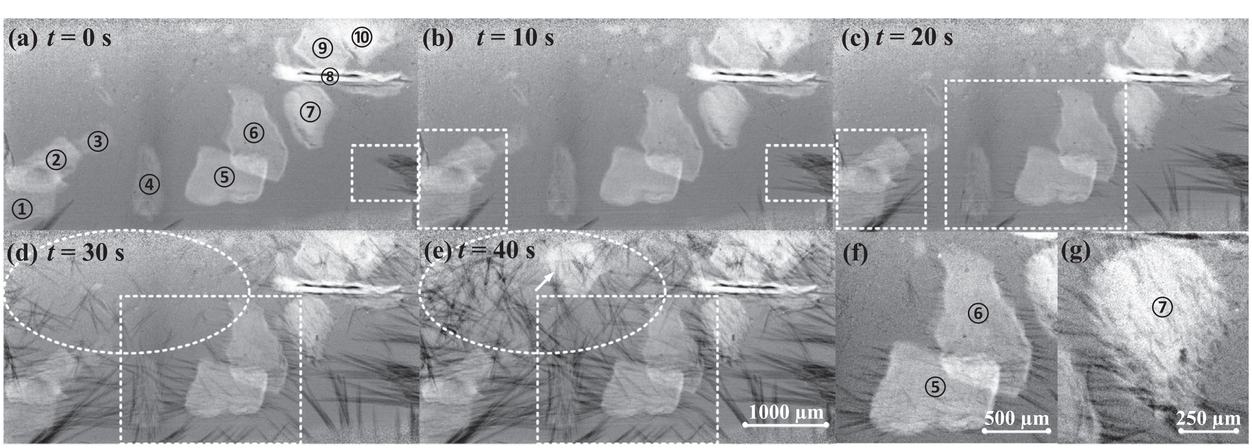

Fig. 2. Images of the primary Al_2Cu intermetallic growth on oxide particles from (a) to (e); The field of view is 5120 × 2624 µm^2 and images were recorded at 1 fps. The t = 0 s frame was set as the frame when the sonotrode was switched off and removed from the melt; (f) An enlarged image of intermetallic growth on oxide particles No. 5 and No. 6 in (d); (g) An enlarged image of intermetallic growth on oxide particle No. 7 in (d).

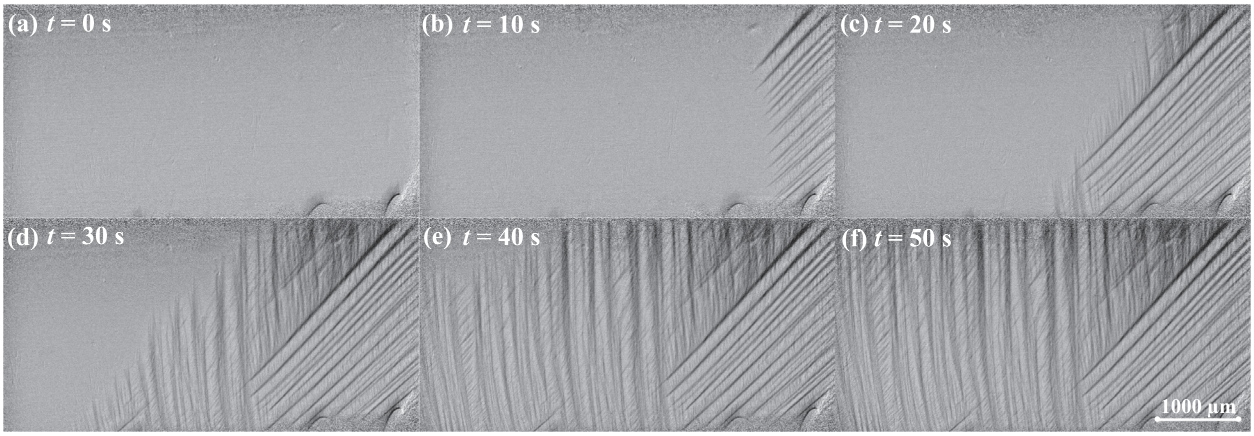

Fig. 3. Images of the primary Al_2Cu intermetallic growth without the presence of aluminium oxide particles in the melt. The field of view is $5120 \times 2624\ \mu m^2$ and images were recorded at 1 fps. The $t = 0$ s frame was set as the frame before the appearance of primary Al_2Cu intermetallic in the field of view.

as $320 \pm 20\ \mu m$. Note that the intermetallic growth on the fragments of oxide film is essentially in three dimensions as can be observed on oxide particle *No. 7* as shown in Fig. 2(g). It is important to point out that a showering of equiaxed primary Al_2Cu intermetallics followed by further equiaxed growth was observed at the top left corner of the field of view as highlighted by a dashed ellipse in Fig. 2(d), and (e). This is a result of prior fragmentation of growing Al_2Cu intermetallic particles by ultrasonic processing and is discussed in detail elsewhere [18].

For comparison, the typical primary Al_2Cu intermetallic growth without prior USP and without fragments of oxide film in the melt is illustrated in Fig. 3. Again, a corresponding Supplementary Video (Supplementary Video 2) is supplied in the online version. The frame before the appearance of primary Al_2Cu intermetallic in the field of view was set as $t = 0$ s. As we can see, without the presence of oxide particles in the melt, the primary Al_2Cu intermetallic grew in the elongated needle-shape, reaching more than 2624 ± 5 $0\ \mu m$ in length.

A comparison between Figs. 2(e) and 3(f) shows significant refinement of primary Al_2Cu intermetallic from more than 2600 μm in length to approximately $320\ \mu m$. This substantiates that enhancing heterogeneous nucleation of primary phase on fragments of oxide film can promote microstructural refinement.

4. Conclusion

In summary, the growth of primary Al_2Cu intermetallic on fragments of oxide film in a hypereutectic Al-35% Cu alloy was clearly observed in-situ and in real time. This direct observation provides conclusive evidence for the longstanding argument that oxide particles in a real metallic alloy melt can act as nucleation substrates for primary phases during solidification. In addition, the significant refinement of primary Al_2Cu intermetallics observed with the presence of oxide particles as compared with those without oxide particles in the melt unambiguously confirms that enhanced heterogeneous nucleation of primary phases on oxide particles can promote structure refinement as has been presumed before based on indirect evidence [3–9].

Acknowledgements

The authors acknowledge financial support from the UK Engineering and Physical Science Research Council (EPSRC) for the Ultra-Cast project [grants EP/L019884/1; EP/L019825/1; EP/L019965/1]. Experiments were performed on the Psiché beamline at Synchrotron SOLEIL, France [Proposal No. 2016076]. Beamline I12 at Diamond Light Source, UK, is also thanked for loan of the high speed camera.

Appendix A. Supplementary data

Supplementary data associated with this article can be found, in the online version, at https://doi.org/10.1016/j.matlet.2017.11.090.

References

[1] J.A. Dantzig, M. Rappaz, Solidification, 1st. ed., EPFL Press, Lausanne, 2009.
[2] W. Kurz, D.J. Fisher, Fundamentals of Solidification, 4th rev. ed., Trans Tech Publications, Zurich, Switzerland, 1998.
[3] G.I. Eskin, D.G. Eskin, Ultrasonic Treatment of Light Alloy Melts, 2nd ed., CRC Press, Boca Raton, Florida, 2015.
[4] G.I. Eskin, Ultrasonic Treatment of Molten Aluminium, Metallurgiya, Moscow, 1988.
[5] Z. Fan, Y. Wang, M. Xia, S. Arumuganathar, Enhanced heterogeneous nucleation in AZ91D alloy by intensive melt shearing, Acta Mater. 57 (2009) 4891–4901.
[6] H.T. Li, Y. Wang, Z. Fan, Mechanisms of enhanced heterogeneous nucleation during solidification in binary Al–Mg alloys, Acta Mater. 60 (2012) 1528–1537.
[7] Y. Wang, H.T. Li, Z. Fan, Oxidation of aluminium alloy melts and inoculation by oxide particles, Trans. Ind. Inst. Met. 65 (2012) 653–661.
[8] Z. Fan, Y. Wang, Z.F. Zhang, M. Xia, H.T. Li, J. Xu, et al., Shear enhanced heterogeneous nucleation in some Mg- and Al-alloys, Int. J. Cast Met. Res. 22 (2009) 318–322.
[9] F. Wang, D. Eskin, J. Mi, T. Connolley, J. Lindsay, M. Mounib, A refining mechanism of primary Al_3Ti intermetallic particles by ultrasonic treatment in the liquid state, Acta Mater. 116 (2016) 354–363.
[10] F. Wang, D. Eskin, T. Connolley, J-w Mi, Influence of ultrasonic treatment on formation of primary Al3Zr in Al–0.4Zr alloy, Trans. Nonferrous Met. Soc. China. 27 (2017) 977–985.
[11] P.D. Lee, J.D. Hunt, Hydrogen porosity in directional solidified aluminium-copper alloys: in situ observation, Acta Mater. 45 (1997) 4155–4169.
[12] R.H. Mathiesen, L. Arnberg, X-ray radiography observations of columnar dendritic growth and constitutional undercooling in an Al–30wt%Cu alloy, Acta Mater. 53 (2005) 947–956.
[13] D. Tan, T.L. Lee, J.C. Khong, T. Connolley, K. Fezzaa, J. Mi, High-speed synchrotron X-ray imaging studies of the ultrasound shockwave and enhanced flow during metal solidification processes, Metall. Mater. Trans. A. 46 (2015) 2851–2861.
[14] W. Mirihanage, W. Xu, J. Tamayo-Ariztondo, D. Eskin, M. Garcia-Fernandez, P. Srirangam, et al., Synchrotron radiographic studies of ultrasonic melt processing of metal matrix nano composites, Mater. Lett. 164 (2016) 484–487.
[15] H. Yasuda, I. Ohnaka, K. Kawasaki, A. Sugiyama, T. Ohmichi, J. Iwane, et al., Direct observation of stray crystal formation in unidirectional solidification of Sn–Bi alloy by X-ray imaging, J. Cryst. Growth. 262 (2004) 645–652.
[16] H. Huang, D. Shu, Y. Fu, J. Wang, B. Sun, Synchrotron radiation X-ray imaging of cavitation bubbles in Al–Cu alloy melt, Ultrason. Sonochem. 21 (2014) 1275–1278.
[17] A. King, N. Guignot, P. Zerbino, E. Boulard, K. Desjardins, M. Bordessoule, et al., Tomography and imaging at the PSICHE beam line of the SOLEIL synchrotron, Rev. Sci. Instrum. 87 (2016) 093704.
[18] F. Wang, T. Connolley, D. Eskin, J. Mi, B. Koe, B. Wang, A synchrotron X-radiography study of primary Al2Cu intermetallic fragmentation and refinement induced by ultrasonic melt processing in an Al-35Cu alloy, Ultrason. Sonochem. (2017), Submitted.